ORIGINAL ARTICLE

Source–sink dynamics assists the maintenance of a pollinating wasp

Xin Tong[1] | Yuan-Yuan Ding[1] | Jun-Yin Deng[1] | Rong Wang[1,2] | Xiao-Yong Chen[1,2]

[1]Zhejiang Tiantong Forest Ecosystem National Observation and Research Station, Shanghai Key Laboratory for Urban Ecological Processes and Eco-Restoration, School of Ecological and Environmental Sciences, East China Normal University, Shanghai, China

[2]Shanghai Institute of Pollution Control and Ecological Security, Shanghai, China

Correspondence
Rong Wang and Xiao-Yong Chen, Zhejiang Tiantong Forest Ecosystem National Observation and Research Station, Shanghai Key Laboratory for Urban Ecological Processes and Eco-Restoration, School of Ecological and Environmental Sciences, East China Normal University, Shanghai, China.
Emails: rwang@des.ecnu.edu.cn (RW); xychen@des.ecnu.edu.cn (X-YC)

Abstract

Dispersal that unites spatially subdivided populations into a metapopulation with source–sink dynamics is crucial for species persistence in fragmented landscapes. Understanding such dynamics for pollinators is particularly urgent owing to the ongoing global pollination crisis. Here, we investigated the population structure and source–sink dynamics of a pollinating wasp (*Wiebesia* sp. 3) of *Ficus pumila* in the Zhoushan Archipelago of China. We found significant asymmetry in the pairwise migrant numbers for 22 of 28 cases on the historical timescale, but only two on the contemporary timescale. Despite a small population size, the sole island not colonized by a superior competitor wasp (*Wiebesia* sp. 1) consistently behaved as a net exporter of migrants, supplying large sinks. Comparable levels of genetic diversity, with few private alleles and low genetic differentiation (total F_{ST}: 0.03; pairwise F_{ST}: 0.0005–0.0791), were revealed among all the islands. There was a significant isolation-by-distance pattern caused mainly by migration between the competition-free island and other islands, otherwise the pattern was negligible. The clustering analysis failed to detect multiple gene pools for the whole region. Thus, the sinks were most probably organized into a patchy population. Moreover, the estimates of effective population sizes were comparable between the two timescales. Thus the source–sink dynamics embedded within a well-connected population network may allow *Wiebesia* sp. 3 to persist at a competitive disadvantage. This study provides evidence that metapopulations in the real world may be complicated and changeable over time, highlighting the necessity to study such metapopulations in detail.

KEYWORDS
asymmetrical gene flow, effective population size, patchy population, pollinating fig wasp, source–sink dynamics

1 | INTRODUCTION

Spatial subdivision characterizes most natural populations as a consequence of heterogeneous-quality habitats (Tscharntke et al., 2012) and/or habitat fragmentation (Potapov et al., 2017; Wang et al., 2011). Migration across unsuitable matrices can unite local populations into a metapopulation. Along with increasing the dispersal among local populations, the metapopulation can be classified into isolated populations, the classical metapopulation, or a patchy population (Dallas et al., 2020). However, migration is usually asymmetrical. Populations in high-quality habitats are more than self-supporting and provide net emigration, while populations in

---

poor-quality habitats are only maintained by net immigration (Furrer & Pasinelli, 2016; Pulliam, 1988). Identifying source populations within a large population network helps target the areas of high priority for conserving vulnerable species (Loreau et al., 2013) and controling invasive species (Dauphinais et al., 2018). Sink areas are nonetheless important for sustaining the whole network by functioning as breeding sites and dispersal stepping-stones (Murphy, 2001), and by increasing spatial asynchrony (Fox et al., 2017). However, studies providing empirical evidence on source–sink populations are surprisingly rare (reviewed by Furrer & Pasinelli, 2016).

There are several difficulties that hinder source–sink assessments. Identifying source and sink populations is often thought to require detailed demographic data, including both directional migration rates among populations and population-specific estimates of reproductive and survival rates (Furrer & Pasinelli, 2016; Runge et al., 2006). However, information on immigration and emigration is generally lacking in field studies (Nystrand et al., 2010). Some studies circumvent this problem by assuming migration has negligible effects on population demography (Boughton, 1999), but this contradicts the tenet of source–sink theory (Pulliam, 1988). Furthermore, traditional capture–recapture approaches commonly used to estimate vital rates are unable to discriminate between mortality and emigration, leading to the underestimation of local survival rates (Paquet et al., 2020). Additionally, those demographic estimates only describe the contemporary source–sink patterns, while source/sink status and strength may vary over time with changing environments (Grof-Tisza et al., 2019; Loreau et al., 2013).

Taking these factors into consideration, genetic techniques may allow for the easier identification of dispersal among spatially subdivided populations (Baguette et al., 2013). Specifically, migration can be estimated both on historical timescales using the distribution of allele frequencies among populations (Slatkin, 1985), and on contemporary timescales by assigning genetic components based on individual multilocus genotypes (Wilson & Rannala, 2003). Combining estimates of current and historical migration then offers perspectives on the long-term stability of population dynamics (Jiang et al., 2021; Palstra et al., 2007). Although it is difficult to infer local demographic rates from genetic data, the importance of local demography in source–sink dynamics may be overstated, because net migrants among populations and local demographic rates necessarily mirror each other if averaged over a long time period (Loreau et al., 2013). Additionally, the distribution of genetic variation within and among local populations and the inferred dispersal patterns provide ways to differentiate the three models of spatial population structure: patchy, meta-, and isolated populations (Mayer et al., 2009). As a consequence, an increasing number of genetic studies have clarified the source–sink states of various vertebrate taxa (Andreasen et al., 2012; Banks et al., 2015; Manier & Arnold, 2005; Minnie et al., 2018; O'Keefe et al., 2009). Nevertheless, insect pollinators have received less attention, especially regarding how genetic connectivity among populations and source–sink dynamics promote their persistence (Franzen & Nilsson, 2013; Iles et al., 2018) under the ongoing global 'pollination crisis' (Burkle et al., 2013; Potts et al., 2010). Such studies

are particularly urgent for highly specialized pollinators, because they are more prone to extinction during environmental changes than generalists and their loss is more likely to drive the extirpation of host plants (Tylianakis, 2013).

With more than 800 species providing abundant figs for a diverse range of vertebrate frugivores, fig trees (*Ficus*, Moraceae) are keystone species in tropical and subtropical regions (Chen et al., 2010; Shanahan et al., 2001). Most *Ficus* species are pollinated by only the females of a single or very few agaonid wasp species, and agaonid larvae, in turn, acquire nutrients from the galled flowers of their host figs, forming obligate mutualisms with high specificity (Cook & Rasplus, 2003; Cruaud et al., 2012; Wang et al., 2021). Although fig wasps, including agaonid wasps and parasitoids, are weak active flyers, they can disperse over long distances using the wind (Ahmed et al., 2009; Harrison, 2003). In general, fig wasps of canopy figs disperse farther than those of understory figs (Harrison & Rasplus, 2006). Thus, the former shows very limited genetic differentiation over expansive geographic areas (Bain et al., 2016; Kobmoo et al., 2010; Molbo et al., 2004; Sutton et al., 2016), whereas the latter may form spatially structured populations (Rodriguez et al., 2017; Tian et al., 2015; Yu et al., 2019). However, if monsoons occur during female-emergence periods, they may enable long-distance and strongly directional dispersal of fig wasps, shaping source–sink population structure. Such a population structure and its ecological implications have not been investigated yet.

Ficus pumila Linn. is one of the most northerly distributed fig trees, with a natural distribution extending from the Ryukyu Islands to China and Vietnam. *Wiebesia pumilae* Hill (Hymenoptera: Agaonidae) was previously thought to be its sole pollinator, but recent molecular data revealed three cryptic pollinators in China, referred to as *Wiebesia* spp. 1, 2, and 3 (Chen et al., 2012). *Wiebesia* spp. 1 and 2 diverged due to the uplift of the Wuyi Mountains and both underwent significant postglacial spatial expansion, shaping their widespread, yet predominantly allopatric, distributions (Chen et al., 2012). By contrast, *Wiebesia* sp. 3 declined in abundance during that period and presently has a very limited distribution, primarily on the offshore islands of the Zhoushan Archipelago where it shares some habitats with *Wiebesia* sp. 1 (Chen et al., 2014). Recent evidence shows that *Wiebesia* sp. 1 has a nearly nonoverlapping earlier emergence phenology than *Wiebesia* sp. 3 (Liu et al., 2014). The foundress first entering a male fig usually lays most or all of the eggs in high-value flowers, thereby reducing the oviposition rates of subsequent foundresses (Dunn, 2020). All else being equal, the phenological difference confers *Wiebesia* sp. 1 a competitive advantage over *Wiebesia* sp. 3. For the latter species, depressed reproductive rates are expected in habitats where have also been colonized by *Wiebesia* sp. 1 (hereafter, "contact habitat"), relative to those habitats solely occupied by *Wiebesia* sp. 3 (hereafter, "noncontact habitat"). According to the source–sink theory (Pulliam, 1988), we hypothesized that: (a) contact habitats receive net flows of immigrants of *Wiebesia* sp. 3 coming from noncontact habitats, and (b) the source–sink dynamics stabilize population sizes of *Wiebesia* sp. 3 that would otherwise decline over a long period due to the asymmetrical competition with *Wiebesia* sp. 1.

To test these hypotheses, we used microsatellites to investigate the spatial genetic structure of *Wiebesia* sp. 3 in the archipelago, and we inferred migration patterns and effective population sizes (N_e) on both contemporary and historical timescales. The historical timescale here corresponds to approximately 600 years ago (~$4N_e$ generations), when the two wasp species had probably already been established in this region (Liu et al., 2014). Specifically, we asked the following questions: (a) Is dispersal among islands symmetrical? Alternatively, is there any island showing net emigration (i.e., serving as the source) or receiving net immigrants (i.e., serving as the sink)? (b) Are the migration patterns consistent between historical and contemporary timescales? (c) Are the effective population sizes similar between the two timescales?

2 | MATERIALS AND METHODS

2.1 | Sample collection

The study was conducted in the Zhoushan Archipelago, which is the largest offshore archipelago in China. During 2015, we investigated the 11 islands where *Wiebesia* sp. 3 was previously found (Chen et al., 2012, 2014), as well as five additional islands; however, no fig trees were found on one island (Daxie). Female *F. pumila* individuals produce figs once a year. The figs are receptive in late April to early May and mature in the autumn in the studied area. The male individuals produce figs twice a year, and the two crops of male figs are receptive in late April to early May and July to August, respectively. *Wiebesia* spp. usually produce two generations annually, which emerge from mature male *F. pumila* figs and quickly enter receptive figs in spring (April–May) and summer (July–August), respectively (Liu et al., 2013, 2014). There are many more mature male figs in the spring than in the summer; therefore, we collected mature male figs, from which wasps were about to emerge, between April and May on the 15 islands (Figure 1) to reduce the adverse impacts of sampling on both wasps and plants. A total of 724 figs were collected and kept in fine-mesh bags to allow adult fig wasps to emerge. The wasps were then stored in absolute ethanol at 4°C. No nonpollinating fig wasps were found in the studied region.

2.2 | DNA extraction and microsatellite genotyping

To reduce the possibility of sampling siblings, we used only 1–3 female wasps per fig (867 wasps from 724 figs) for the experiments. Total genomic DNA was extracted from the fig wasps using the method of Liu et al. (2013) and genotyped using nine microsatellite loci (*WP076*, *WP197*, *WP231*, *WP294*, *WP304*, *WP399*, *WP403*, *WP447* and *WP522*). PCR was conducted following the protocol of Liu et al. (2009). The PCR products were separated and scanned on an ABI 3730 DNA Analyser (Applied Biosystems). Allele sizes were scored using GENEMAPPER v.4.0 with post hoc manual examinations.
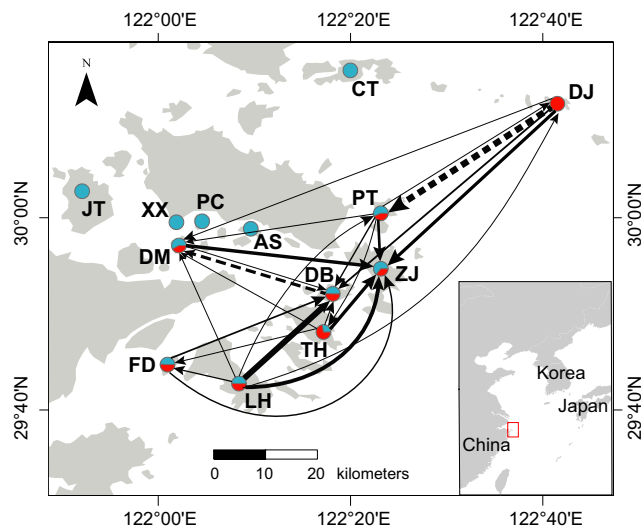
FIGURE 1 Sample locations of the pollinating wasps of *Ficus pumila* in the Zhoushan Archipelago of China, and pairwise source–sink relationships of *Wiebesia* sp. 3. Dashed and solid arrows indicate the directionality of contemporary and long-term gene flow, respectively, with thickness scaled by the net number of migrants per generation (except for the contemporary migration from DJ to PT, which is too large to show). The relative proportions of *Wiebesia* sp. 1 (blue) and sp. 3 (red) within each site are also presented [Colour figure can be viewed at wileyonlinelibrary.com]

The two cryptic wasp species co-occurring on the archipelago, *Wiebesia* spp. 1 and 3, are morphologically indistinguishable. However, substantial differences in allele size ranges were found between the two species at *WP294* (129–157 bp in *Wiebesia* sp. 1 vs. 113 bp in *Wiebesia* sp. 3), and can be used to determine species identity (Liu et al., 2014). We also confirmed this approach by sequencing the mtDNA *COI* genes of 90 wasps and comparing those sequences with the haplotypes from Chen et al. (2012). The analysis revealed a 100% identification of the wasp species on the basis of the *WP294* locus. Therefore, we used the *WP294* locus to identify the species of the remaining wasps. Finally, 321 samples of *Wiebesia* sp. 3 were obtained from 241 figs on eight islands (Table 1), and the only pure population (DJ) was free from competition with *Wiebesia* sp. 1 (Figure 1). Only those samples of *Wiebesia* sp. 3 were used in the subsequent analyses, and their *WP294* locus was not further included because of monomorphism in this species.

2.3 | Estimation of genetic diversity

The software MICRO-CHECKER v.2.2.3 (van Oosterhout et al., 2004) was used to screen for stuttering, large allele dropout, and possible null alleles. An F_{ST}-outlier analysis implemented in FDIST2 (Beaumont & Nichols, 1996) was performed to identify loci that were potentially under selection. Deviations from Hardy–Weinberg equilibrium and linkage disequilibrium between loci were determined using GENEPOP v.4.2.1 (Rousset, 2008), with threshold significance levels

TABLE 1 Sample size and genetic diversity estimates as well as results of the bottleneck tests for each site

Site	n	A	R_A	R_{PA}	H_O	H_E	F_{IS}	Wilcoxon test[a]	Mode-shift test
DB	36	5.63 (1.30)	5.43 (1.29)	0.00 (0.00)	0.586 (0.101)	0.678 (0.097)	0.137	0.47	L-shaped
DJ	35	5.13 (2.17)	5.02 (2.06)	0.03 (0.06)	0.469 (0.128)	0.627 (0.111)	0.256	0.68	L-shaped
DM	34	5.25 (1.58)	5.18 (1.54)	0.16 (0.32)	0.634 (0.196)	0.649 (0.126)	0.023	0.63	L-shaped
FD	34	6.25 (1.91)	6.09 (1.84)	0.22 (0.39)	0.616 (0.121)	0.714 (0.053)	0.139	0.63	L-shaped
LH	30	7.63 (1.51)	7.57 (1.50)	1.09 (1.07)	0.634 (0.124)	0.706 (0.095)	0.103	0.98	L-shaped
PT	33	6.00 (1.69)	5.87 (1.70)	0.36 (0.43)	0.518 (0.145)	0.672 (0.108)	0.232	0.81	L-shaped
TH	85	6.88 (1.81)	5.83 (1.64)	0.20 (0.36)	0.637 (0.076)	0.695 (0.072)	0.085	0.81	L-shaped
ZJ	34	6.38 (1.60)	6.20 (1.51)	0.03 (0.04)	0.625 (0.103)	0.710 (0.084)	0.122	0.37	L-shaped

Note: Values in parentheses are the standard deviations of the estimates across loci.

Abbreviations: A, number of alleles per locus; F_{IS}, inbreeding coefficient; H_e, expected heterozygosity; H_O, observed heterozygosity; n, sample size; R_A, allelic richness per locus rarefied to the minimum sample size; R_{PA}, private allelic richness.

[a]p-value of one-tailed Wilcoxon signed-rank test for heterozygosity excess under the two-phase mutation model (TPM).

for multiple comparisons adjusted using the sequential Bonferroni method (Rice, 1989).

The genetic diversity on each island was measured using the mean number of alleles per locus (A) and allelic richness (R_A) rarefied to the minimum sample size implemented in FSTAT v.2.9.3 (Goudet, 2001), and by private allelic richness (R_{PA}) estimated in HP-RARE v.1.0 (Kalinowski, 2005), as well as by observed (H_O) and expected (H_e) heterozygosities calculated in ARLEQUIN v.3.5 (Excoffier & Lischer, 2010). Inbreeding coefficients (F_{IS}) were also estimated for each island in FSTAT.

2.4 | Analysis of population structure

Genetic differentiation was measured for all and paired islands using multilocus F_{ST} values in accordance with Weir and Cockerham (1984) and implemented in FSTAT, with significance tested by permuting genotypes among samples 1000 times. Because of the possibility of DJ serving as the source for others (hypothesis 1), we determined the isolation-by-distance (IBD) patterns for three cases: among all eight islands, among the seven islands without DJ, and between DJ and the seven islands. The IBD patterns were examined using Mantel tests in the first two cases, and a linear regression in the third case, between $F_{ST}/(1-F_{ST})$ and the natural logarithm of the geographical distance, as suggested by Rousset (1997). Mantel tests were performed with 9999 permutations using the R package "vegan" (Oksanen et al., 2019).

Potential population structure was investigated using the Bayesian genetic clustering approach in STRUCTURE v.2.3.3 (Pritchard et al., 2000). Ten independent analyses were run for each potential number of clusters (K) ranging from 1 to 10, with each run having 10^6 Markov chain Monte Carlo (MCMC) iterations following a burnin period of 10^5 steps. The admixture model allowing for correlated allele frequencies was used (Falush et al., 2003). In accordance with Wang (2017), we used both the logarithm of the posterior probability of the data for each K, $\ln P(D|K)$ (Pritchard et al., 2000), and the second

order rate of change of the likelihood, ΔK (Evanno et al., 2005), to identify the most likely number of genetic clusters. The program CLUMPP (Jakobsson & Rosenberg, 2007) was employed to average the results over 10 replicates.

2.5 | Analysis of source–sink dynamics

We assessed short- and long-term source–sink dynamics through contemporary and historical migration patterns, respectively. Bidirectional migration rates between all pairs of islands were estimated allowing asymmetry. Gene flow via other islands was not considered, though it might influence source/sink status by the stepping-stone type metapopulation, particularly over long time-scales. To provide a detailed picture of source–sink dynamics, we first identified sources and sinks in a pairwise manner. Any island that had significantly more immigrants than emigrants would be defined as a sink. Thus, the same island could be classified as both a source and a sink, depending on which other islands it was compared with. Finally, we evaluated the overall source–sink status for each island by its net flow of migrants with respect to all other islands, to understand the islands' roles in the source–sink dynamics.

2.5.1 | Contemporary timescale

Contemporary migration rates were estimated using a Bayesian approach implemented in BAYESASS v.3.0.4 (Wilson & Rannala, 2003). To achieve optimal parameter mixing, we initially adjusted the mixing parameters (Δ_A, Δ_F, and Δ_M) so that their acceptance rates reached between 20% and 60%. With the finalized parameters, MCMC was run for 5×10^7 iterations including a burnin period of 5×10^6, and parameters were sampled every 500 iterations. Owing to the common nonconvergence problems of MCMC chains (Meirmans, 2014), we performed 10 repeat runs of the analyses with different

random seeds and selected the best-fit run as indicated by the lowest Bayesian deviance for further analyses.

BAYESASS is unable to directly estimate emigration, which nevertheless can be determined from immigration rates while correcting for unequal population sizes (Wilson & Rannala, 2003). The contemporary effective population sizes were estimated using the single-sample method on the basis of linkage disequilibrium and implemented in NEESTIMATOR v.2.1 (Do et al., 2014), which excluded rare alleles at $P_{crit} = 0.02$ to achieve a good balance between precision and accuracy for the estimation (Waples & Do, 2010). With estimates of population size and immigration rate, we determined the migrant numbers for all pairs of islands in both directions. To assess significance of asymmetry for pairwise migrant numbers, we estimated the 95% confidence intervals (CIs) using the standard deviation of the marginal posterior distribution for immigration rate.

2.5.2 | Historical timescale

We performed maximum-likelihood (ML) analyses in accordance with the coalescent theory in MIGRATE v.3.6.11 (Beerli, 2006) to estimate long-term gene flow. Ten short chains of 5×10^4, with a sampling interval of 100 steps, and three long chains of 5×10^6 genealogies, recorded every 1000 steps were run for each analysis. To explore genealogical space more efficiently, we employed Markov coupled MCMC (i.e., MC^3) using an adaptive heating scheme at temperatures of 1.0, 1.2, 1.5 and 3.0. The Brownian motion approximation of the stepwise mutation model was implemented using a constant mutation rate across loci. Runs were repeated until posterior probabilities stabilized, where F_{ST}-based estimates of θ and M were used as the starting values in the first run and subsequent runs, respectively, using the ML estimates from each previous run as the starting parameters. ML estimates along with 95% CIs from the final run were reported and used.

MIGRATE provides estimates for the scaled parameters $\theta = 4N_e\mu$ (μ, mutation rate per generation) and $M = m/\mu$ (m, immigration rate per generation). We calculated the effective number of migrants per generation ($N_e m$) from i to j using $\theta_j \times M_{i \to j}/4$. Similar to the contemporary estimation, we obtained a 95% CI for $N_e m$ only when considering the uncertainty in the estimation of migration rate. To facilitate comparisons with contemporary estimates, we converted θ and M into the unscaled parameters N_e and m, respectively, by approaching the estimation of μ using the method of Turner et al. (2002). Specifically, we treated each island as a replicate estimate of the relative mutation rates across loci. For each island, we set $\mu = 1 \times 10^{-3}$ for the locus with the highest θ, and then scaled other loci in accordance with $\mu_i/\mu_{max} = \theta_i/\theta_{max}$, to provide the upper limit of μ. Similarly, the lower-bound estimate of μ was obtained by setting $\mu = 1 \times 10^{-5}$ for the locus with the lowest θ, and we scaled other loci using $\mu_i/\mu_{min} = \theta_i/\theta_{min}$. The average of the scaled mutation rates over all the loci was used for the conversion. Estimates were compared between the two timescales using a pairwise Mann–Whitney test

for N_e and using Mantel tests with 9999 permutations for m and $N_e m$.

3 | RESULTS

3.1 | Within-island genetic variation

Most loci were successfully amplified, with rates ranging from 97.2% (WP522) to 100% (WP231 and WP294), and an overall rate of 98.8%. The locus WP294 showed monomorphism in Wiebesia sp. 3, and thus was used only to determine species identity and excluded from further analyses. All the other loci were polymorphic with 6–13 alleles, and an average of 10.25 ± 2.25 standard deviation alleles per locus. Excess homozygosity was found using MICRO-CHECKER at all the loci, but it was not consistent across islands for any locus (occurring in 1–3 populations). This may have resulted from inbreeding rather than null alleles, because few foundresses lay eggs in a single fig, and their offspring have a high possibility to mate with siblings, as supported by the detection of inbreeding in each island (Table 1). No stuttering or large allele dropout was detected. FDIST2 did not indicate any F_{ST}-outliers, suggesting selective neutrality for the loci. Significant linkage disequilibrium was found in only one of 224 pairwise tests among islands (between WP403 and WP522 in DB). We detected significant deviations from Hardy–Weinberg equilibrium in five out of 64 tests, occurring at five loci and in three islands.

The indices of genetic diversity for each island are provided in Table 1. Either the average number of alleles per locus (A) or allelic richness (R_A) did not differ significantly across islands, except that they were higher in LH than in DB, DJ, and DM ($p < .05$). The observed heterozygosity (H_O) was significantly lower in DJ relative to FD, LH, and TH, while minor differences were found between all the other pairwise island comparisons. There was no significant difference in expected heterozygosity (H_E) across islands. The private allelic richness (R_{PA}) was generally low, except in LH.

3.2 | Population structure

Weak genetic differentiation was observed among islands, as revealed by low global F_{ST} (0.03 ± 0.007) and pairwise F_{ST}, ranging from 0.0005 (DB vs. LH) to 0.0791 (DJ vs. FD), despite most values being statistically significant ($p < .05$). Pairwise F_{ST} values between DJ and other islands were significantly higher than those between islands, excluding DJ (Figure 2a). There was a significant IBD pattern among all the islands ($r = .496$, $p = .005$), but it became negligible when DJ was excluded from the Mantel test ($r = .278$, $p = .118$; Figure 2b). This suggested that DJ was genetically different from the other islands and had relatively limited genetic exchange with them. This was also supported by a significant positive correlation between genetic differentiation and geographic distance for DJ-involved pairwise comparisons ($r = .806$, $p = .029$; Figure 2b).
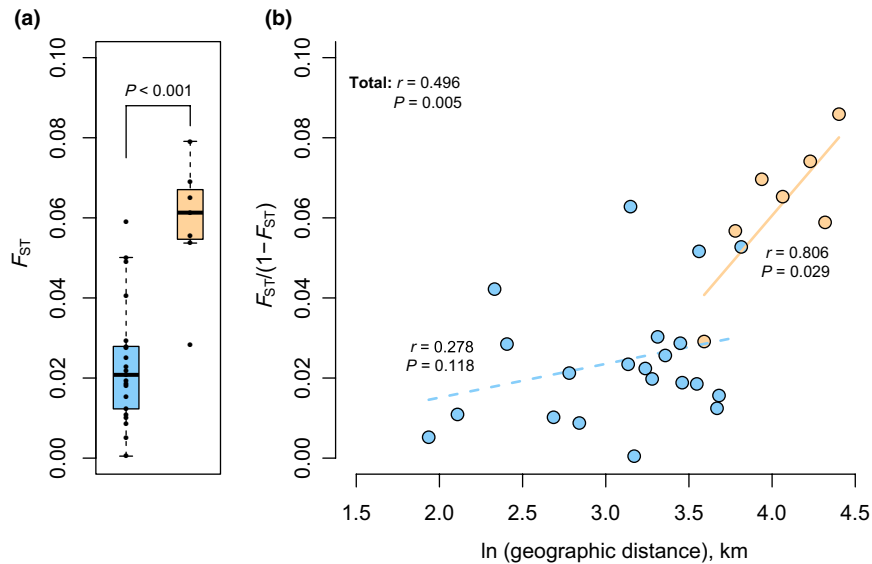
FIGURE 2 Genetic differentiation between pairwise populations. (a) The F_{ST} estimates were significantly higher between DJ and other seven populations (the orange boxplot) than among the populations excluding DJ (the blue boxplot). (b) Relationships between $F_{ST}/(1-F_{ST})$ and log-transformed geographic distance. Significant isolation-by-distance patterns were found among all populations as well as between DJ and other seven populations (orange circles), but not among the populations excluding DJ (blue circles) [Colour figure can be viewed at wileyonlinelibrary.com]
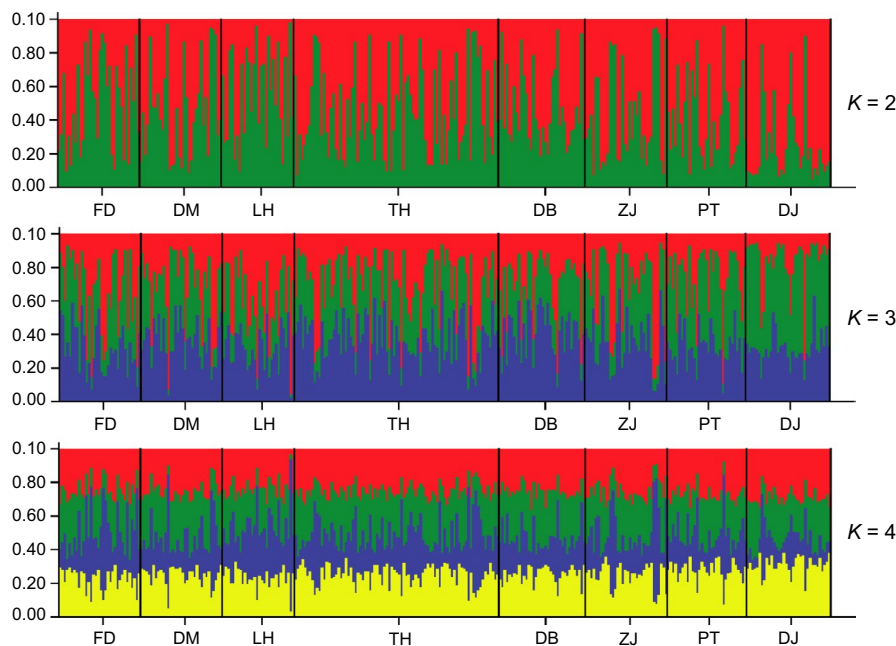
FIGURE 3 Assignment of individuals to multiple candidate genetic clusters of $K = 2$–4 by the STRUCTURE analyses. Each vertical line represents one individual. Populations are arranged from west to east [Colour figure can be viewed at wileyonlinelibrary.com]

The genetic clustering analysis performed in STRUCTURE showed an almost random change in $\ln P(D|K)$ with increasing K, and the ΔK statistic was small (around 1–8) for each $K \geq 2$ (Figure S1), suggesting that there was only one genetic cluster. For different values of K, each individual showed an admixture of all the K clusters, and all the islands were assigned to each cluster to similar extents (Figure 3), which also indicated that all the individuals belonged to a single gene pool.

3.3 | Source–sink dynamics

3.3.1 | Contemporary patterns

The BAYESASS run with the lowest Bayesian deviance indicated a substantial proportion of immigrants (8.4%–32.5% with an average of 24.5%) in each island. All the other runs with different

random seeds showed consistent results with that run (maximum difference = 0.09), basically eliminating the possibility of MCMC being trapped in a local mode. Immigration rates between all pairs of islands ranged from 0.4% (PT into TH) to 21.3% (DB into DM), with an average of 3.5%, and were mostly symmetrical with overlapping 95% CIs (Table 2). We detected significant asymmetrical migration rates from DB to DM, from DJ to PT, and from TH to FD, LH and ZJ, with nonsignificant migration occurring in the reverse directions. For emigration, we corrected for unequal population sizes using the point estimates of N_e from NEESTIMATOR, which ranged from 12.9 (DM) to 1340.8 (PT) with an average of 324.7 (Table 2). Two island pairs showed significant asymmetry in the number of migrants per generation (Figure 1): DB had slightly more emigrants to DM (2.8, 95% CI = 1.6–3.9) than immigrants from DM (0.3, 95% CI = 0–0.8), while DJ had a surprisingly large number of emigrants to PT (229.4, 95% CI = 95.9–362.9) in contrast to few immigrants

TABLE 2 Contemporary estimates of effective population size (N_e), pairwise immigration rates, and overall net numbers of immigrants

Site	N_e	Immigration rates from								Net number of immigrants
		DB	DJ	DM	FD	LH	PT	TH	ZJ	
DB	25.4	0.769 (0.708, 0.830)	0.014 (0, 0.039)	0.010 (0, 0.030)	0.013 (0, 0.037)	0.011 (0, 0.031)	0.008 (0, 0.022)	0.167 (0.098, 0.237)	0.008 (0, 0.024)	−82.5 (−226.9, 8.9)
DJ	60.4	0.012 (0, 0.034)	0.901 (0.845, 0.958)	0.029 (0, 0.062)	0.010 (0, 0.031)	0.010 (0, 0.029)	0.008 (0, 0.023)	0.022 (0, 0.062)	0.008 (0, 0.024)	−248.7 (−429.3, −80.0)
DM	12.9	**0.213 (0.124, 0.302)**	0.015 (0, 0.045)	0.688 (0.658, 0.718)	0.018 (0, 0.049)	0.012 (0, 0.034)	0.008 (0, 0.024)	0.038 (0, 0.115)	0.009 (0, 0.026)	−36.5 (−105.9, 7.7)
FD	169.4	0.041 (0, 0.112)	0.018 (0, 0.052)	0.020 (0, 0.052)	0.731 (0.667, 0.794)	0.017 (0, 0.045)	0.008 (0, 0.023)	**0.156 (0.06, 0.253)**	0.009 (0, 0.030)	12.5 (−78.5, 95.9)
LH	112.1	0.100 (0.001, 0.199)	0.039 (0, 0.098)	0.014 (0, 0.040)	0.013 (0, 0.038)	0.681 (0.653, 0.710)	0.013 (0, 0.035)	**0.126 (0.017, 0.235)**	0.014 (0, 0.038)	13.8 (−61.1, 76.6)
PT	1340.8	0.025 (0, 0.064)	**0.171 (0.072, 0.271)**	0.021 (0, 0.055)	0.017 (0, 0.044)	0.010 (0, 0.029)	0.675 (0.659, 0.691)	0.073 (0, 0.168)	0.009 (0, 0.025)	429.1 (76.7, 879.8)
TH	859.0	0.038 (0, 0.109)	0.020 (0, 0.053)	0.006 (0, 0.018)	0.008 (0, 0.023)	0.005 (0, 0.015)	0.004 (0, 0.011)	0.916 (0.834, 0.998)	0.004 (0, 0.012)	−74.8 (−310.4, 191.1)
ZJ	17.9	0.057 (0, 0.121)	0.019 (0, 0.053)	0.009 (0, 0.028)	0.057 (0.008, 0.105)	0.010 (0, 0.030)	0.008 (0, 0.023)	**0.164 (0.085, 0.243)**	0.676 (0.656, 0.695)	−13.0 (−53.7, 10.8)

Note: The immigration rate from a population to itself refers to the proportion of nonmigrants within that population. Significant asymmetry of migration rate with nonoverlapping 95% CI is denoted by bold (marking the larger value), and significant asymmetry of migrant number (that is, with unequal population sizes accounted for) with nonoverlapping 95% CI is indicated by grey areas (on the major direction of gene flow).

TABLE 3 Historical estimates of unscaled effective population size (N_e), pairwise immigration rate (m), and overall net numbers of immigrants

| Site | N_e | Immigration rates (m, $\times 10^{-3}$) from | | | | | | | | Net number of immigrants |
		DB	DJ	DM	FD	LH	PT	TH	ZJ	
DB	536.9 (492.5, 586.7)	–	4.43 (3.94, 4.96)	7.32 (6.68, 7.99)	6.39 (5.80, 7.02)	14.00 (13.12, 14.92)	4.17 (3.70, 4.68)	4.91 (4.4, 5.47)	**7.48 (6.84, 8.16)**	10.2 (6.5, 14.1)
DJ	166.8 (137.0, 181.1)	5.50 (4.80, 6.27)	–	3.61 (3.05, 4.24)	**10.01 (9.05, 11.03)**	8.65 (7.76, 9.61)	13.41 (12.3, 14.59)	4.89 (4.23, 5.61)	**8.32 (7.45, 9.26)**	−3.5 (−5.9, −1.1)
DM	287.6 (262.9, 315.4)	**11.15 (10.23, 12.12)**	4.12 (3.58, 4.72)	–	6.13 (5.46, 6.86)	6.30 (5.62, 7.03)	5.45 (4.82, 6.13)	8.14 (7.36, 8.97)	**9.80 (8.94, 10.71)**	−0.3 (−3.4, 2.7)
FD	273.0 (252.1, 296.4)	7.69 (6.96, 8.47)	5.59 (4.97, 6.26)	5.04 (4.45, 6.33)	–	8.58 (7.81, 9.41)	3.58 (3.09, 4.12)	**6.19 (5.53, 6.90)**	7.44 (6.72, 8.21)	−1.2 (−3.9, 1.7)
LH	141.1 (130.6, 152.7)	**20.70 (19.36, 22.11)**	7.23 (6.45, 8.08)	**8.02 (7.19, 8.90)**	9.49 (8.59, 10.45)	–	9.94 (9.02, 10.92)	**12.66 (11.62, 13.77)**	7.83 (7.01, 8.70)	−10.0 (−12.8, −7.3)
PT	118.5 (109.2, 128.8)	**9.68 (8.65, 10.78)**	12.63 (11.45, 13.88)	6.51 (5.68, 7.42)	**7.79 (6.87, 8.78)**	**16.07 (14.74, 17.48)**	–	7.64 (6.73, 8.62)	**7.94 (7.02, 8.95)**	−4.6 (−6.9, −2.4)
TH	171.6 (159.2, 185.3)	**10.23 (9.28, 11.24)**	6.11 (5.39, 6.89)	9.67 (8.75, 10.65)	5.31 (4.64, 6.04)	9.48 (8.57, 10.45)	7.51 (6.71, 8.38)	–	**11.03 (10.05, 12.07)**	−4.5 (−7.0, −1.9)
ZJ	739.6 (670.1, 819.1)	5.23 (4.73, 5.76)	5.27 (4.77, 5.80)	7.42 (6.83, 8.05)	4.27 (3.82, 4.75)	5.52 (5.01, 6.06)	4.03 (3.60, 4.50)	6.04 (5.51, 6.61)	–	13.7 (9.7, 17.9)

Note: N_e and m were estimated from scaled parameters θ and M by $N_e = \theta/4\mu$ and $m = M \times \mu$, respectively, using $\mu = 3.77 \times 10^{-4}$ obtained by averaging across scaled estimates of μ for each microsatellite. Significant asymmetry of migration rate with nonoverlapping 95% CI is denoted by marking the larger value in bold, and significant asymmetry of migrant number with nonoverlapping 95% CI is indicated by grey areas on the major direction of gene flow.

from PT (0.5, 95% CI = 0–1.4). The overall analysis indicated that DJ was a net source and PT was a net sink, while the six other islands did not show any significant net emigration or immigration levels (Table 2).

3.3.2 | Historical patterns

Coalescent estimates of effective population size (N_e) ranged from 118.5 (PT) to 739.6 (ZJ) with an average of 304.4 (Table 3), and these values were comparable with the contemporary estimates (Mann–Whitney $U = 14$, $p = .641$). Between all pairs of islands, long-term migration rates (m) ranged from 0.4% (PT into FD) to 2.1% (DB into LH) with an average of 0.8% (Table 3), and the number of migrants ($N_e m$) varied from 0.6 (DM into DJ) to 7.5 (LH into DB) with an average of 2.1. The Mantel tests comparing m or $N_e m$ between long-term and contemporary timescales did not reveal any significant correlations (m: $r = .149$, $p = .252$; $N_e m$: $r = −.453$, $p = .925$). Asymmetrical m and asymmetrical $N_e m$ were found in 17 and 22, respectively, of 28 pairwise comparisons between islands (Table 3). However, the predominant directions of migration were reversed for the two types of asymmetry within the same island pair. For example, a significantly higher m was found from ZJ to any other island than in the reverse direction, but when accounting for the relatively large population size of ZJ, the comparison of $N_e m$ revealed that ZJ received more migrants than it provided (significant for six out of seven pairwise tests, Table 3). The pairwise source–sink relationships are shown in Figure 1, where the same island being both a source and a sink was frequently observed. The overall analysis identified ZJ and DB as net sinks, and classified LH, PT, TH, and DJ as net sources (Table 3).

4 | DISCUSSION

Two or more pollinating wasps have been increasingly found in the same fig species (Yang et al., 2015), violating the one-to-one rule of fig–wasp mutualisms (Wiebes, 1979). Local coexistence in general seems difficult for cryptic fig wasp species (Darwell & Cook, 2017). In *F. pumila*, two pollinating wasp species, *Wiebesia* spp. 1 and 3, are found in sympatry on some islands of the Zhoushan Archipelago, whereas *Wiebesia* sp. 1 has a competitive advantage over *Wiebesia* sp. 3 (Liu et al., 2014). Our results suggest that the *Wiebesia* sp. 3 populations are maintained by source–sink dynamics. The competition-free island functions as a refuge for *Wiebesia* sp. 3, and that population serves as a substantial source fuelling other islands. Those sinks are well connected with each other by high dispersal rates of the wasps, which further reduces local extinction risks. This study provides an empirical test for source–sink dynamics in pollinators, and may offer a regional view—complementary to those possible local mechanisms (e.g., Montero-Pau & Serra, 2011; Zhang et al., 2004)—for understanding cryptic species coexistence.

4.1 | Asymmetric gene flow and source–sink dynamics

The migration analyses revealed significant asymmetry of gene flow between pairs of islands. Although the migration patterns changed over time (discussed later), the island DJ, which is not colonized by *Wiebesia* sp. 1, was consistently identified as a source across historical and contemporary timescales. The major migration direction from DJ to the other islands may be correlated with the occurrences of monsoons in this region. The emergence and dispersal of the wasps occurred predominantly from April to May and from July to August (Liu et al., 2014), when the prevailing winds blow from ocean (east) to continent (west) in East China. Because fig wasps disperse over long distances passively by the wind (Harrison, 2003; Harrison & Rasplus, 2006), the monsoon patterns suggest that *Wiebesia* spp. can readily migrate from the easternmost island (DJ) to the others, whereas migration in the opposite direction is much more difficult. This may explain why the DJ population consistently acts as a source for *Wiebesia* sp. 3, and why *Wiebesia* sp. 1 has not colonized DJ.

In contrast to the asymmetrical gene flow trend from large to small populations, as revealed by previous studies (Hansen et al., 2007; Manier & Arnold, 2005), large populations predominantly behaved as sinks (e.g., PT on the contemporary scale and DB and ZJ on the historical scale), whereas the consistent source (DJ) had a relatively small population size on both timescales (Tables 2 and 3). Although counterintuitive, this pattern is not contradictory to the tenet of the source–sink theory, which states that asymmetrical dispersal arises owing to differences in habitat qualities (and thus, reproductive rates) rather than population size imbalance (Pulliam, 1988). Indeed, local abundance may be decoupled from habitat quality when habitats are linked by dispersal (Iles et al., 2018; Van Horne, 1983). In some cases, sinks are buoyed demographically by immigration, making them larger than the sources (Andreasen et al., 2012; Weegman et al., 2016). Thus, without clear information regarding the relevant processes (birth, death, immigration, and emigration), population size may be a poor predictor of source–sink status (Runge et al., 2006).

Instead, our results suggest that the source–sink dynamics of *Wiebesia* sp. 3 are most probably driven by interspecific competition. There are more *F. pumila* figs that provide potential breeding sites for their pollinating wasps in the sink habitats than in the source, but the presence of *Wiebesia* sp. 1 in the sinks may dramatically undermine the habitat quality, as perceived by *Wiebesia* sp. 3 (Liu et al., 2014), through niche destruction (Kylafis & Loreau, 2011). In this manner, the presence of superior competitors turns a good habitat into a bad one, and a potential source into a sink (termed "soft sink", sensu Schmidt et al., 2000). Immigration from refuge populations may rescue the inferior competitor from extinction in soft sinks, if the migrants are surplus individuals who do not contribute to the local reproduction of sources (Amarasekare & Nisbet, 2001). This spatial storage effect provides a foundation for the mass-effect paradigm of species coexistence in metacommunities (Leibold et al.,

2004; O'Sullivan et al., 2019), and it has also been empirically documented in other animal systems (Dubart et al., 2019; Jones et al., 2014; Lindegren et al., 2014). However, if migration causes large costs to the reproduction of sources, source populations may not sustain themselves, leading to the regional exclusion of the species (Amarasekare, 2003). The latter case is almost impossible in fig wasps, because only a small portion of mated females enter figs and lay their eggs (Dunn, 2020). Therefore, it can be expected that the source–sink dynamics promote the persistence of *Wiebesia* sp. 3, which is also supported by the stability of the population size across timescales. Alternatively, competition between very similar species may not be sufficiently intense to cause species exclusion, but it alters the densities of their local populations instead, which is termed "density compensation" (Lara et al., 2020; MacArthur et al., 1972). However, because the competitive advantage of *Wiebesia* sp. 1 over *Wiebesia* sp. 3 has direct relevance to reproduction (Liu et al., 2014), it may be difficult for the two species to live together for many generations through density compensation.

Our results also showed that the opposite conclusion would be drawn for the direction of gene flow and source–sink status if the relative population sizes were not considered (Table 3). Few previous studies have measured migration asymmetry by directly comparing estimates of migration rate (m) from programs such as MIGRATE or BAYESASS between the two directions of a population pair, whereby they further determined sources and sinks (Andreasen et al., 2012; Chiucchi & Gibbs, 2010; DeSilva & Dodd, 2020; Palstra et al., 2007), but see Manier and Arnold (2005) and Sonsthagen et al. (2012). Technically speaking, whether a population acts as a source or a sink depends on the difference between its immigration and emigration rates, whereas m represents the immigration rates of different populations. Overlooking this difference may generate misleading inferences for asymmetrical migration and lead to the misidentification of sources in conservation planning, particularly when populations differ greatly in size (Wilson & Rannala, 2003).

4.2 | Patchy population structure and dispersal ability

The sinks most likely form a patchy population instead of a classical metapopulation. The genetic clustering analysis indicated that all the islands belonged to a single genetic cluster, and the descriptive statistics showed comparable genetic diversity across sinks with a generally low richness of private alleles. Moreover, pairwise genetic differentiation was predominantly low (0.0005–0.0591), with considerable migration rates among sinks. All these results suggest high genetic connectivity among the sinks. Moreover, no isolation-by-distance pattern was found in the sinks, while IBD should be expected in a classical metapopulation (Mayer et al., 2009). Therefore, despite the de facto difficulty in clearly distinguishing between classical metapopulations and patchy populations because they represent a continuum (Mayer et al., 2009; Rasic & Keyghobadi, 2012),

the spatial structure of *Wiebesia* sp. 3 is more akin to that of a patchy population. Consistent with this conclusion, weak genetic differentiation was revealed among the host populations in the Zhoushan Archipelago (Chen et al., 2008).

The lack of a spatial genetic structure for *Wiebesia* sp. 3 among the sinks probably reflects its ability to disperse over distances of tens of kilometers, which contrasts with previous studies that suggested the localized dispersal of dioecious-fig pollinators (Harrison, 2003; Harrison & Rasplus, 2006). Many dioecious figs are understory shrubs and have high population densities, resulting in long-distance dispersal not be required and active pollinator dispersal beneath the tree canopy being the probable rule (Harrison & Rasplus, 2006). However, *F. pumila* dwells in open areas (mostly rocks and abandoned walls) or reaches forest canopies by creeping up large trees, presumably allowing its pollinators to use the wind for long-distance dispersal, like many monoecious-fig wasps (Cooper et al., 2020; Kobmoo et al., 2010; Sutton et al., 2016). Low genetic differentiation and a lack of IBD over distances of more than 1000 km have indeed been revealed for *Wiebesia* sp. 2 (Liu et al., 2015).

4.3 | Comparison between the timescales

The directionality of gene flow and the source–sink states of local populations did not exhibit temporal consistency, but showed some reversals across timescales instead. Such changes were not surprising, because the selection pressure and demography underlying source–sink dynamics are likely to fluctuate over the long term (Boughton, 1999; Grof-Tisza et al., 2019). Here, environmental and demographic stochasticity levels might cause substantial temporal variations in the numbers of *F. pumila* trees and their figs, particularly because those habitats are fragmented by a completely hostile matrix (i.e., the sea). These variations may not only have directly impacted the demography of *Wiebesia* sp. 3, but they may also have altered the selection pressure from competition with *Wiebesia* sp. 1. Furthermore, changes in wind direction and speed during the emergence periods of the pollinating wasps may also affect the dispersal direction and distance. The ultimate instability of population dynamics probably reflects the interactions of these processes.

Another notable result from the comparison between timescales (cf. Tables 2 and 3) was the apparent difference in the magnitudes of the estimated migration rate. However, this cannot be regarded as an increase in gene flow, because the coalescent estimate of the migration rate describes only effective movements contributing to the establishment of alleles under the offsetting effects of drift (Beerli & Felsenstein, 2001), while contemporary timescales do not allow drift to function exhaustively and the migration may include alleles that will be ultimately lost under a migration–drift equilibrium (Wilson & Rannala, 2003). Larger contemporary estimates than coalescent estimates can be expected, and results from directly comparing the two estimates should be interpreted with caution (e.g., Chiucchi & Gibbs, 2010).

5 | CONCLUSIONS

The discovery of cryptic fig-pollinating wasp species in sympatry raises the question of how ecologically similar cryptic species coexist. Our study on the pollinating wasps of *F. pumila* indicates that the local populations of *Wiebesia* sp. 3 with reproductive rates depressed by a sympatric cryptic wasp are fuelled by immigrants from the competition-free refuge population. High dispersal rates of the wasps join the sinks to form a patchy population, further reducing the local extinction risk. This spatial structure having source–sink dynamics may contribute to the persistence of the wasp species facing asymmetrical competition. Moreover, some source and sink populations show reverse trends across time. These findings demonstrate that metapopulations in the real world are complicated, and they highlight that such metapopulations should be studied using detailed approaches.

AUTHOR CONTRIBUTIONS
Xiao-Yong Chen conceived and designed the study. Yuan-Yuan Ding carried out the experiments. Xin Tong, Yuan-Yuan Ding and Rong Wang analysed the data. Xin Tong produced the figures. Xin Tong wrote the manuscript with the assistance of Xiao-Yong Chen, Jun-Yin Deng, and Rong Wang. All the authors reviewed the manuscript.

DATA AVAILABILITY STATEMENT
Data from this study have been deposited in the Dryad Digital Repository: https://doi.org/10.5061/dryad.r4xgxd2bc.

ORCID
Xin Tong https://orcid.org/0000-0002-3474-3043
Xiao-Yong Chen https://orcid.org/0000-0002-4795-8940

REFERENCES
Ahmed, S., Compton, S. G., Butlin, R. K., & Gilmartin, P. M. (2009). Wind-borne insects mediate directional pollen transfer between desert fig trees 160 kilometers apart. *Proceedings of the National Academy of Sciences of the United States of America*, 106(48), 20342–20347. https://doi.org/10.1073/pnas.0902213106

Amarasekare, P. (2003). Competitive coexistence in spatially structured environments: A synthesis. *Ecology Letters*, 6(12), 1109–1122. https://doi.org/10.1046/j.1461-0248.2003.00530.x

Amarasekare, P., & Nisbet, R. M. (2001). Spatial heterogeneity, source-sink dynamics, and the local coexistence of competing species. *American Naturalist*, 158(6), 572–584. https://doi.org/10.1086/323586

Andreasen, A. M., Stewart, K. M., Longland, W. S., Beckmann, J. P., & Forister, M. L. (2012). Identification of source-sink dynamics in mountain lions of the Great Basin. *Molecular Ecology*, 21(23), 5689–5701. https://doi.org/10.1111/j.1365-294X.2012.05740.x

Baguette, M., Blanchet, S., Legrand, D., Stevens, V. M., & Turlure, C. (2013). Individual dispersal, landscape connectivity and ecological

networks. *Biological Review*, *88*, 310–326. https://doi.org/10.1111/brv.12000

Bain, A., Borges, R. M., Chevallier, M. H., Vignes, H., Kobmoo, N., Peng, Y. Q., Cruaud, A., Rasplus, J. Y., Kjellberg, F., & Hossaert-Mckey, M. (2016). Geographic structuring into vicariant species-pairs in a wide-ranging, high-dispersal plant–insect mutualism: The case of *Ficus racemosa* and its pollinating wasps. *Evolutionary Ecology*, *30*(4), 663–684. https://doi.org/10.1007/s10682-016-9836-5

Banks, S. C., Lorin, T., Shaw, R. E., McBurney, L., Blair, D., Blyton, M. D., Smith, A. L., Pierson, J. C., & Lindenmayer, D. B. (2015). Fine-scale refuges can buffer demographic and genetic processes against short-term climatic variation and disturbance: A 22-year case study of an arboreal marsupial. *Molecular Ecology*, *24*(15), 3831–3845. https://doi.org/10.1111/mec.13279

Beaumont, M. A., & Nichols, R. A. (1996). Evaluating loci for use in the genetic analysis of population structure. *Proceedings of the Royal Society B: Biological Sciences*, *263*(1377), 1619–1626. https://doi.org/10.1098/rspb.1996.0237

Beerli, P. (2006). Comparison of Bayesian and maximum-likelihood inference of population genetic parameters. *Bioinformatics*, *22*(3), 341–345. https://doi.org/10.1093/bioinformatics/bti803

Beerli, P., & Felsenstein, J. (2001). Maximum likelihood estimation of a migration matrix and effective population sizes in n subpopulations by using a coalescent approach. *Proceedings of the National Academy of Sciences of the United States of America*, *98*(8), 4563–4568. https://doi.org/10.1073/pnas.081068098

Boughton, D. A. (1999). Empirical evidence for complex source–sink dynamics with alternative states in a butterfly metapopulation. *Ecology*, *80*(8), 2727–2739. https://doi.org/10.1890/0012-9658(1999)080[2727:EEFCSS]2.0.CO;2

Burkle, L. A., Marlin, J. C., & Knight, T. M. (2013). Plant-pollinator interactions over 120 years: Loss of species, co-occurrence, and function. *Science*, *339*(6127), 1611–1615. https://doi.org/10.1126/science.1232728

Chen, Y., Compton, S. G., Liu, M., & Chen, X. Y. (2012). Fig trees at the northern limit of their range: The distributions of cryptic pollinators indicate multiple glacial refugia. *Molecular Ecology*, *21*(7), 1687–1701. https://doi.org/10.1111/j.1365-294X.2012.05491.x

Chen, Y., Li, H. Q., Liu, M., & Chen, X. Y. (2010). Species-specificity and coevolution of figs and their pollinating wasps. *Biodiversity Science*, *18*(1), 1–10. https://doi.org/10.3724/SP.J.1003.2010.001

Chen, Y., Liu, M., Compton, S. G., & Chen, X. Y. (2014). Distribution of nuclear mitochondrial pseudogenes in three pollinator fig wasps associated with *Ficus pumila*. *Acta Oecologica*, *57*, 142–149. https://doi.org/10.1016/j.actao.2013.10.001

Chen, Y., Shi, M. M., Ai, B., Gu, J. M., & Chen, X. Y. (2008). Genetic variation in island and mainland populations of *Ficus pumila* (Moraceae) in eastern Zhejiang of China. *Symbiosis*, *45*(1–3), 37–44.

Chiucchi, J. E., & Gibbs, H. L. (2010). Similarity of contemporary and historical gene flow among highly fragmented populations of an endangered rattlesnake. *Molecular Ecology*, *19*(24), 5345–5358. https://doi.org/10.1111/j.1365-294X.2010.04860.x

Cook, J. M., & Rasplus, J. Y. (2003). Mutualists with attitude: Coevolving fig wasps and figs. *Trends in Ecology & Evolution*, *18*(5), 241–248. https://doi.org/10.1016/S0169-5347(03)00062-4

Cooper, L., Bunnefeld, L., Hearn, J., Cook, J. M., Lohse, K., & Stone, G. N. (2020). Low-coverage genomic data resolve the population divergence and gene flow history of an Australian rain forest fig wasp. *Molecular Ecology*, *29*(19), 3649–3666. https://doi.org/10.1111/mec.15523

Cruaud, A., Rønsted, N., Chantarasuwan, B., Chou, L. S., Clement, W. L., Couloux, A., Cousins, B., Genson, G., Harrison, R. D., Hanson, P. E., Hossaert-Mckey, M., Jabbour-Zahab, R., Jousselin, E., Kerdelhué, C., Kjellberg, F., Lopez-Vaamonde, C., Peebles, J., Peng, Y.-Q., Pereira, R. A. S., … Savolainen, V. (2012). An extreme case of plant–insect codiversification: Figs and fig-pollinating wasps. *Systematic Biology*, *61*(6), 1029–1047. https://doi.org/10.1093/sysbio/sys068.

Dallas, T. A., Saastamoinen, M., Schulz, T., & Ovaskainen, O. (2020). The relative importance of local and regional processes to metapopulation dynamics. *Journal of Animal Ecology*, *89*(3), 884–896. https://doi.org/10.1111/1365-2656.13141

Darwell, C. T., & Cook, J. M. (2017). Cryptic diversity in a fig wasp community—Morphologically differentiated species are sympatric but cryptic species are parapatric. *Molecular Ecology*, *26*(3), 937–950. https://doi.org/10.1111/mec.13985

Dauphinais, J. D., Miller, L. M., Swanson, R. G., & Sorensen, P. W. (2018). Source–sink dynamics explain the distribution and persistence of an invasive population of common carp across a model Midwestern watershed. *Biological Invasions*, *20*(8), 1961–1976. https://doi.org/10.1007/s10530-018-1670-y

DeSilva, R., & Dodd, R. S. (2020). Fragmented and isolated: Limited gene flow coupled with weak isolation by environment in the paleoendemic giant sequoia (*Sequoiadendron giganteum*). *American Journal of Botany*, *107*(1), 45–55. https://doi.org/10.1002/ajb2.1406

Do, C., Waples, R. S., Peel, D., Macbeth, G. M., Tillett, B. J., & Ovenden, J. R. (2014). NEESTIMATOR v2: Re-implementation of software for the estimation of contemporary effective population size (N_e) from genetic data. *Molecular Ecology Resources*, *14*(1), 209–214. https://doi.org/10.1111/1755-0998.12157

Dubart, M., Pantel, J. H., Pointier, J. P., Jarne, P., & David, P. (2019). Modeling competition, niche, and coexistence between an invasive and a native species in a two-species metapopulation. *Ecology*, *100*(6), e02700. https://doi.org/10.1002/ecy.2700

Dunn, D. W. (2020). Stability in fig tree-fig wasp mutualisms: How to be a cooperative fig wasp. *Biological Journal of the Linnean Society*, *130*(1), 1–17. https://doi.org/10.1093/biolinnean/blaa027

Evanno, G., Regnaut, S., & Goudet, J. (2005). Detecting the number of clusters of individuals using the software STRUCTURE: A simulation study. *Molecular Ecology*, *14*(8), 2611–2620. https://doi.org/10.1111/j.1365-294X.2005.02553.x

Excoffier, L., & Lischer, H. E. L. (2010). Arlequin suite ver 3.5: A new series of programs to perform population genetics analyses under Linux and Windows. *Molecular Ecology Resources*, *10*(3), 564–567. https://doi.org/10.1111/j.1755-0998.2010.02847.x

Falush, D., Stephens, M., & Pritchard, J. K. (2003). Inference of population structure using multilocus genotype data: Linked loci and correlated allele frequencies. *Genetics*, *164*(4), 1567–1587. https://doi.org/10.1093/genetics/164.4.1567

Fox, J. W., Vasseur, D., Cotroneo, M., Guan, L. L., & Simon, F. (2017). Population extinctions can increase metapopulation persistence. *Nature Ecology & Evolution*, *1*(9), 1271–1278. https://doi.org/10.1038/s41559-017-0271-y

Franzen, M., & Nilsson, S. G. (2013). High population variability and source–sink dynamics in a solitary bee species. *Ecology*, *94*(6), 1400–1408. https://doi.org/10.1890/11-2260.1

Furrer, R. D., & Pasinelli, G. (2016). Empirical evidence for source–sink populations: A review on occurrence, assessments and implications. *Biological Reviews*, *91*(3), 782–795. https://doi.org/10.1111/brv.12195

Goudet, J. (2001). *FSTAT, a program to estimate and test gene diversities and fixation indices, version 2.9.3*. http://www2.unil.ch/popgen/softwares/fstat.htm

Grof-Tisza, P., Pepi, A., Holyoak, M., & Karban, R. (2019). Precipitation-dependent source–sink dynamics in a spatially-structured population of an outbreaking caterpillar. *Landscape Ecology*, *34*(5), 1131–1143. https://doi.org/10.1007/s10980-019-00793-z

Hansen, M. M., Skaala, O., Jensen, L. F., Bekkevold, D., & Mensberg, K. L. D. (2007). Gene flow, effective population size and selection at major histocompatibility complex genes: Brown trout in the Hardanger Fjord, Norway. *Molecular Ecology*, *16*(7), 1413–1425. https://doi.org/10.1111/j.1365-294X.2007.03255.x

Harrison, R. D. (2003). Fig wasp dispersal and the stability of a keystone plant resource in Borneo. *Proceedings of the Royal Society B-Biological Sciences*, 270, S76–S79. https://doi.org/10.1098/rsbl.2003.0018

Harrison, R. D., & Rasplus, J. Y. (2006). Dispersal of fig pollinators in Asian tropical rain forests. *Journal of Tropical Ecology*, 22, 631–639. https://doi.org/10.1017/S0266467406003488

Iles, D. T., Williams, N. M., & Crone, E. E. (2018). Source-sink dynamics of bumblebees in rapidly changing landscapes. *Journal of Applied Ecology*, 55(6), 2802–2811. https://doi.org/10.1111/1365-2664.13175

Jakobsson, M., & Rosenberg, N. A. (2007). CLUMPP: A cluster matching and permutation program for dealing with label switching and multimodality in analysis of population structure. *Bioinformatics*, 23(14), 1801–1806. https://doi.org/10.1093/bioinformatics/btm233

Jiang, K., Tong, X., Ding, Y.-Q., Wang, Z.-W., Miao, L.-Y., Xiao, Y.-E., Huang, W.-C., Hu, Y.-H., Chen, X.-Y., & Gillespie, R. (2021). Shifting roles of the East China Sea in the phylogeography of red nanmu in East Asia. *Journal of Biogeography*, in press https://doi.org/10.1111/jbi.14215

Jones, J. A., Harris, M. R., & Siefferman, L. (2014). Physical habitat quality and interspecific competition interact to influence territory settlement and reproductive success in a cavity nesting bird. *Frontiers in Ecology and Evolution*, 2, 71. https://doi.org/10.3389/fevo.2014.00071

Kalinowski, S. T. (2005). HP-RARE 1.0: A computer program for performing rarefaction on measures of allelic richness. *Molecular Ecology Notes*, 5(1), 187–189. https://doi.org/10.1111/j.1471-8286.2004.00845.x

Kobmoo, N., Hossaert-McKey, M., Rasplus, J. Y., & Kjellberg, F. (2010). *Ficus racemosa* is pollinated by a single population of a single agaonid wasp species in continental South-East Asia. *Molecular Ecology*, 19(13), 2700–2712. https://doi.org/10.1111/j.1365-294X.2010.04654.x.

Kylafis, G., & Loreau, M. (2011). Niche construction in the light of niche theory. *Ecology Letters*, 14(2), 82–90. https://doi.org/10.1111/j.1461-0248.2010.01551.x

Lara, C., Curiel-Duran, H. A., & Castillo-Guevara, C. (2020). Coexistence among morphologically similar hummingbird species is promoted via density compensation in a Mexican temperate forest. *Ecological Research*, 35(2), 416–427. https://doi.org/10.1111/1440-1703.12090.

Leibold, M. A., Holyoak, M., Mouquet, N., Amarasekare, P., Chase, J. M., Hoopes, M. F., Holt, R. D., Shurin, J. B., Law, R., Tilman, D., Loreau, M., & Gonzalez, A. (2004). The metacommunity concept: A framework for multi-scale community ecology. *Ecology Letters*, 7(7), 601–613. https://doi.org/10.1111/j.1461-0248.2004.00608.x

Lindegren, M., Andersen, K. H., Casini, M., & Neuenfeldt, S. (2014). A metacommunity perspective on source–sink dynamics and management: The Baltic Sea as a case study. *Ecological Applications*, 24(7), 1820–1832. https://doi.org/10.1890/13-0566.1

Liu, M., Compton, S. G., Peng, F. E., Zhang, J., & Chen, X. Y. (2015). Movements of genes between populations: Are pollinators more effective at transferring their own or plant genetic markers? *Proceedings of the Royal Society B: Biological Sciences*, 282(1808), 20150290. https://doi.org/10.1098/rspb.2015.0290

Liu, M., Wang, X. Y., Cui, M. Y., & Chen, Y. (2009). Fifteen polymorphic microsatellite loci in *Wiebesia pumilae* (Hill) (Agaonidae). *Conservation Genetics Resources*, 1(1), 189–191. https://doi.org/10.1007/s12686-009-9046-3

Liu, M., Zhang, J., Chen, Y., Compton, S. G., & Chen, X. Y. (2013). Contrasting genetic responses to population fragmentation in a coevolving fig and fig wasp across a mainland-island archipelago. *Molecular Ecology*, 22(17), 4384–4396. https://doi.org/10.1111/mec.12406

Liu, M., Zhao, R., Chen, Y., Zhang, J., Compton, S. G., & Chen, X. Y. (2014). Competitive exclusion among fig wasps achieved via entrainment of host plant flowering phenology. *PLoS One*, 9(5), e97783. https://doi.org/10.1371/journal.pone.0097783

Loreau, M., Daufresne, T., Gonzalez, A., Gravel, D., Guichard, F., Leroux, S. J., Loeuille, N., Massol, F., & Mouquet, N. (2013). Unifying sources and sinks in ecology and Earth sciences. *Biological Reviews*, 88(2), 365–379. https://doi.org/10.1111/brv.12003

MacArthur, R. H., Diamond, J. M., & Karr, J. R. (1972). Density compensation in island faunas. *Ecology*, 53(2), 330–342. https://doi.org/10.2307/1934090

Manier, M. K., & Arnold, S. J. (2005). Population genetic analysis identifies source–sink dynamics for two sympatric garter snake species (*Thamnophis elegans* and *Thamnophis sirtalis*). *Molecular Ecology*, 14(13), 3965–3976. https://doi.org/10.1111/j.1365-294X.2005.02734.x

Mayer, C., Schiegg, K., & Pasinelli, G. (2009). Patchy population structure in a short-distance migrant: Evidence from genetic and demographic data. *Molecular Ecology*, 18(11), 2353–2364. https://doi.org/10.1111/j.1365-294X.2009.04200.x

Meirmans, P. G. (2014). Nonconvergence in Bayesian estimation of migration rates. *Molecular Ecology Resources*, 14(4), 726–733. https://doi.org/10.1111/1755-0998.12216

Minnie, L., Zalewski, A., Zalewska, H., & Kerley, G. I. H. (2018). Spatial variation in anthropogenic mortality induces a source–sink system in a hunted mesopredator. *Oecologia*, 186(4), 939–951. https://doi.org/10.1007/s00442-018-4072-z

Molbo, D., Machado, C. A., Herre, E. A., & Keller, L. (2004). Inbreeding and population structure in two pairs of cryptic fig wasp species. *Molecular Ecology*, 13(6), 1613–1623. https://doi.org/10.1111/j.1365-294X.2004.02158.x

Montero-Pau, J., & Serra, M. (2011). Life-cycle switching and coexistence of species with no niche differentiation. *PLoS One*, 6(5), e20314. https://doi.org/10.1371/journal.pone.0020314

Murphy, M. T. (2001). Source-sink dynamics of a declining Eastern Kingbird population and the value of sink habitats. *Conservation Biology*, 15(3), 737–748. https://doi.org/10.1046/j.1523-1739.2001.015003737.x

Nystrand, M., Griesser, M., Eggers, S., & Ekman, J. (2010). Habitat-specific demography and source–sink dynamics in a population of Siberian jays. *Journal of Animal Ecology*, 79(1), 266–274. https://doi.org/10.1111/j.1365-2656.2009.01627.x

O'Keefe, K., Ramakrishnan, U., van Tuinen, M., & Hadly, E. A. (2009). Source–sink dynamics structure a common montane mammal. *Molecular Ecology*, 18(23), 4775–4789. https://doi.org/10.1111/j.1365-294X.2009.04382.x

Oksanen, J., Blanchet, F. G., Friendly, M., Kindt, R., Legendre, P., McGlinn, D., Minchin, P. R., O'Hara, R. B., Simpson, G. L., Solymos, P., Stevens, M. H. H., Szoecs, E., & Wagner, H. (2019). *vegan: Community ecology package*. R package version 2.5-6. https://CRAN.R-project.org/package=vegan

O'Sullivan, J. D., Knell, R. J., & Rossberg, A. G. (2019). Metacommunity-scale biodiversity regulation and the self-organised emergence of macroecological patterns. *Ecology Letters*, 22(9), 1428–1438. https://doi.org/10.1111/ele.13294

Palstra, F. P., O'Connell, M. F., & Ruzzante, D. E. (2007). Population structure and gene flow reversals in Atlantic salmon (*Salmo salar*) over contemporary and long-term temporal scales: Effects of population size and life history. *Molecular Ecology*, 16(21), 4504–4522. https://doi.org/10.1111/j.1365-294X.2007.03541.x

Paquet, M., Arlt, D., Knape, J., Low, M., Forslund, P., & Part, T. (2020). Why we should care about movements: Using spatially explicit integrated population models to assess habitat source–sink dynamics. *Journal of Animal Ecology*, 89(12), 2922–2933. https://doi.org/10.1111/1365-2656.13357

Potapov, P., Hansen, M. C., Laestadius, L., Turubanova, S., Yaroshenko, A., Thies, C., Smith, W., Zhuravleva, I., Komarova, A., Minnemeyer, S., & Esipova, E. (2017). The last frontiers of wilderness: Tracking loss of intact forest landscapes from 2000 to 2013. *Science Advances*, 3(1), e1600821. https://doi.org/10.1126/sciadv.1600821

Potts, S. G., Biesmeijer, J. C., Kremen, C., Neumann, P., Schweiger, O., & Kunin, W. E. (2010). Global pollinator declines: Trends, impacts and

drivers. *Trends in Ecology & Evolution*, *25*(6), 345–353. https://doi.org/10.1016/j.tree.2010.01.007

Pritchard, J. K., Stephens, M., & Donnelly, P. (2000). Inference of population structure using multilocus genotype data. *Genetics*, *155*(2), 945–959. https://doi.org/10.1093/genetics/155.2.945

Pulliam, H. R. (1988). Sources, sinks, and population regulation. *American Naturalist*, *132*, 652–661. https://doi.org/10.1086/284880

Rasic, G., & Keyghobadi, N. (2012). The pitcher plant flesh fly exhibits a mixture of patchy and metapopulation attributes. *Journal of Heredity*, *103*(5), 703–710. https://doi.org/10.1093/jhered/ess040

Rice, W. R. (1989). Analyzing tables of statistical tests. *Evolution*, *43*(1), 223–225. https://doi.org/10.2307/2409177

Rodriguez, L. J., Bain, A., Chou, L.-S., Conchou, L., Cruaud, A., Gonzales, R., Hossaert-McKey, M., Rasplus, J.-Y., Tzeng, H.-Y., & Kjellberg, F. (2017). Diversification and spatial structuring in the mutualism between *Ficus septica* and its pollinating wasps in insular South East Asia. *BMC Evolutionary Biology*, *17*, 207. https://doi.org/10.1186/s12862-017-1034-8

Rousset, F. (1997). Genetic differentiation and estimation of gene flow from *F*-statistics under isolation by distance. *Genetics*, *145*, 1219–1228.

Rousset, F. (2008). GENEPOP'007: A complete re-implementation of the GENEPOP software for Windows and Linux. *Molecular Ecology Resources*, *8*(1), 103–106. https://doi.org/10.1111/j.1471-8286.2007.01931.x

Runge, J. P., Runge, M. C., & Nichols, J. D. (2006). The role of local populations within a landscape context: Defining and classifying sources and sinks. *American Naturalist*, *167*(6), 925–938. https://doi.org/10.1086/503531

Schmidt, K. A., Earnhardt, J. M., Brown, J. S., & Holt, R. D. (2000). Habitat selection under temporal heterogeneity: Exorcizing the ghost of competition past. *Ecology*, *81*(9), 2622–2630. https://doi.org/10.1890/0012-9658(2000)081[2622:Hsuthe]2.0.Co;2

Shanahan, M., So, S., Compton, S. G., & Corlett, R. (2001). Fig-eating by vertebrate frugivores: A global review. *Biological Reviews*, *76*(4), 529–572. https://doi.org/10.1017/S1464793101005760

Slatkin, M. (1985). Gene flow in natural populations. *Annual Review of Ecology and Systematics*, *16*, 393–430. https://doi.org/10.1146/annurev.es.16.110185.002141

Sonsthagen, S. A., McClaren, E. L., Doyle, F. I., Titus, K., Sage, G. K., Wilson, R. E., Gust, J. R., & Talbot, S. L. (2012). Identification of metapopulation dynamics among Northern Goshawks of the Alexander Archipelago, Alaska, and Coastal British Columbia. *Conservation Genetics*, *13*(4), 1045–1057. https://doi.org/10.1007/s10592-012-0352-z

Sutton, T. L., Riegler, M., & Cook, J. M. (2016). One step ahead: A parasitoid disperses farther and forms a wider geographic population than its fig wasp host. *Molecular Ecology*, *25*(4), 882–894. https://doi.org/10.1111/mec.13445

Tian, E. W., Nason, J. D., Machado, C. A., Zheng, L. N., Yu, H., & Kjellberg, F. (2015). Lack of genetic isolation by distance, similar genetic structuring but different demographic histories in a fig-pollinating wasp mutualism. *Molecular Ecology*, *24*(23), 5976–5991. https://doi.org/10.1111/mec.13438

Tscharntke, T., Tylianakis, J. M., Rand, T. A., Didham, R. K., Fahrig, L., Batáry, P., Bengtsson, J., Clough, Y., Crist, T. O., Dormann, C. F., Ewers, R. M., Fründ, J., Holt, R. D., Holzschuh, A., Klein, A. M., Kleijn, D., Kremen, C., Landis, D. A., Laurance, W., … Westphal, C. (2012). Landscape moderation of biodiversity patterns and processes - eight hypotheses. *Biological Reviews*, *87*(3), 661–685. https://doi.org/10.1111/j.1469-185X.2011.00216.x

Turner, T. F., Wares, J. P., & Gold, J. R. (2002). Genetic effective size is three orders of magnitude smaller than adult census size in an abundant, estuarine-dependent marine fish (*Sciaenops ocellatus*). *Genetics*, *162*(3), 1329–1339.

Tylianakis, J. M. (2013). The global plight of pollinators. *Science*, *339*(6127), 1532–1533. https://doi.org/10.1126/science.1235464

Van Horne, B. (1983). Density as a misleading indicator of habitat quality. *The Journal of Wildlife Management*, *47*(4), 893–901. https://doi.org/10.2307/3808148

van Oosterhout, C., Hutchinson, W. F., Wills, D. P. M., & Shipley, P. (2004). MICRO-CHECKER: Software for identifying and correcting genotyping errors in microsatellite data. *Molecular Ecology Notes*, *4*(3), 535–538. https://doi.org/10.1111/j.1471-8286.2004.00684.x

Wang, J. L. (2017). The computer program STRUCTURE for assigning individuals to populations: Easy to use but easier to misuse. *Molecular Ecology Resources*, *17*(5), 981–990. https://doi.org/10.1111/1755-0998.12650

Wang, R., Compton, S. G., & Chen, X. Y. (2011). Fragmentation can increase spatial genetic structure without decreasing pollen-mediated gene flow in a wind-pollinated tree. *Molecular Ecology*, *20*(21), 4421–4432. https://doi.org/10.1111/j.1365-294X.2011.05293.x

Wang, R., Yang, Y., Jing, Y. I., Segar, S. T., Zhang, Y. U., Wang, G., Chen, J., Liu, Q.-F., Chen, S., Chen, Y., Cruaud, A., Ding, Y.-Y., Dunn, D. W., Gao, Q., Gilmartin, P. M., Jiang, K., Kjellberg, F., Li, H.-Q., Li, Y.-Y., … Chen, X.-Y. (2021). Molecular mechanisms of mutualistic and antagonistic interactions in a plant-pollinator association. *Nature Ecology & Evolution*, *5*(7), 974–986. https://doi.org/10.1038/s41559-021-01469-1

Waples, R. S., & Do, C. (2010). Linkage disequilibrium estimates of contemporary N_e using highly variable genetic markers: A largely untapped resource for applied conservation and evolution. *Evolutionary Applications*, *3*(3), 244–262. https://doi.org/10.1111/j.1752-4571.2009.00104.x

Weegman, M. D., Bearhop, S., Fox, A. D., Hilton, G. M., Walsh, A. J., McDonald, J. L., & Hodgson, D. J. (2016). Integrated population modelling reveals a perceived source to be a cryptic sink. *Journal of Animal Ecology*, *85*(2), 467–475. https://doi.org/10.1111/1365-2656.12481

Weir, B. S., & Cockerham, C. C. (1984). Estimating *F*-statistics for the analysis of population structure. *Evolution*, *38*(6), 1358–1370. https://doi.org/10.1111/j.1558-5646.1984.tb05657.x

Wiebes, J. T. (1979). Co-evolution of figs and their insect pollinators. *Annual Review of Ecology and Systematics*, *10*, 1–12. https://doi.org/10.1146/annurev.es.10.110179.000245

Wilson, G. A., & Rannala, B. (2003). Bayesian inference of recent migration rates using multilocus genotypes. *Genetics*, *163*, 1177–1191. https://doi.org/10.1093/genetics/163.3.1177

Yang, L. Y., Machado, C. A., Dang, X. D., Peng, Y. Q., Yang, D. R., Zhang, D. Y., & Liao, W. J. (2015). The incidence and pattern of copollinator diversification in dioecious and monoecious figs. *Evolution*, *69*, 294–304. https://doi.org/10.1111/evo.12584

Yu, H., Tian, E., Zheng, L., Deng, X., Cheng, Y., Chen, L., Wu, W., Tanming, W., Zhang, D., Compton, S. G., & Kjellberg, F. (2019). Multiple parapatric pollinators have radiated across a continental fig tree displaying clinal genetic variation. *Molecular Ecology*, *28*(9), 2391–2405. https://doi.org/10.1111/mec.15046

Zhang, D. Y., Lin, K., & Hanski, I. (2004). Coexistence of cryptic species. *Ecology Letters*, *7*(3), 165–169. https://doi.org/10.1111/j.1461-0248.2004.00569.x

SUPPORTING INFORMATION

Additional supporting information may be found online in the Supporting Information section.